2011

Simulations of Vapor/Ice Dynamics in a Freeze-Dryer Condenser

Arnab Ganguly
Purdue University

A Venkattraman
Purdue University

Alina A. Alexeenko
Purdue University - Main Campus, alexeenk@purdue.edu

Simulations of Vapor/Ice Dynamics in a Freeze-Dryer Condenser

Arnab Ganguly, A. Venkattraman, and Alina A. Alexeenko School of Aeronautics and Astronautics, Purdue University, West Lafayette, IN 47907 USA

Abstract. Freeze-drying is a low-pressure, low-temperature condensation pumping process widely used in the manufacture of pharmaceuticals for removal of solvents by sublimation. Key performance characteristics of a freeze-dryer condenser are largely dependent on the vapor and ice dynamics in the low-pressure environment. The main objective of this work is to develop a modeling and computational framework for analysis of vapor and ice dynamics in such freeze-dryer condensers. The direct Simulation Monte Carlo (DSMC) technique is applied to model the relevant physical processes that accompany the vapor flow in the condenser chamber. Low-temperature water vapor molecular model is applied in the DSMC solver SMILE to simulate the flowfield structure. The developing ice front is tracked based on the mass flux computed at the nodes of the DSMC surface mesh. Verification of ice accretion simulations has been done by comparison with analytical free-molecular solutions. Simulations of ice buildup on the coils of a laboratory-scale dryer have been compared with experiments. The comparison shows that unsteady simulations are necessary to reproduce experimentally observed icing structures. The DSMC simulations demonstrate that by tailoring the condenser topology to the flow-field structure of the water vapor jet expanding into a low-pressure reservoir, it is possible to significantly increase water vapor removal rates and improve the overall efficiency of freeze-drying process.

Keywords: DSMC, ice accretion, water vapor flows, freeze-drying
PACS: 51.10.+y

INTRODUCTION

Among the common drying operations, freeze drying is the most expensive [1]. There are significant challenges in making this process efficient. Each freeze drying cycle can last up to 3 days and may consume up to 1.5 million BTU of energy [2]. The high energy expenditures lead to a cost that is 4-8 times higher than other forms of drying [3-5]. During the drying stage, the pressure in the chamber is reduced to near vacuum while the temperature of the shelves is increased. This provides the energy necessary for sublimation. An equation for the drying rate during the ice sublimation stage of the process was derived on the basis of the molecular-kinetic theory of gases by Guigo and Tsvetkov [6] and by Luikov and Lebedev [7]. There exists a delicate balance between heat and mass transfer. If this balance is disturbed, adverse effects could lead to a collapse of the product [8]. Analysis of the mechanism of heat and mass transfer was done by Lebedev where experimental studies of the temperature fields over a permeable plate during ice-water sublimation were investigated [9]. The sublimation rate of an ice disk resting on a heated plate under low pressures was determined by Tachiwaki, et al to measure the variation of the sublimation rates as a function of the thickness and radius of the ice disk [10]. Measurements to determine the accommodation coefficient of water vapor were performed by Kramers and Stemerding [11]. It was shown that in the operating temperatures between -40 to -60C, the accommodation coefficient is close to unity. The vapor formed by sublimation in the product chamber flows into the condenser and condenses to ice. The vapor transport in the condenser depends strongly on the geometric configuration. Oetjen and Haseley proposed guidelines for a good condenser design [12].

Condensers used today are often inefficient due to their large volumes and non-uniformity in vapor condensation. Figure 1 shows the non-uniform ice formation over the coils of the Lyostar dryer after a 50 hour drying run under a 500 mL load. The chamber pressure was maintained at 70 mTorr while the shelf temperature was -15 C. On the coil closest to the duct exit, there is higher ice accumulation and reduces as we move away. Moreover, on the coil farthest away from the duct, being closer to the refrigerant outlet is at a higher temperature and receives no ice accumulation. The thickness of the ice formed on the coil closest to the duct exit is about 2 cm. The vapor removing performance of a dryer is a function of the chamber pressure $Q_m(P_d)$ [13]. According to Kobayashi, the efficiency of the vapor condensing system depends on the geometry of the refrigerated plates/coils [14]. According to Oetjen, the thickness of the ice layer should not exceed 1 cm [12]. The presence of permanent gases also increases non-uniformity [15]. Improving the uniformity of ice formation presents design challenges that have not been addressed to date.

Thus, it is clear that there is a large set of variables that govern the performance of a freeze-drying condenser. An improved understanding of the flow physics is needed to develop optimal designs. The current work uses the

27th International Symposium on Rarefied Gas Dynamics, 2010
AIP Conf. Proc. 1333, 254-259 (2011); doi: 10.1063/1.3562657

DSMC technique to solve the flow field structure in the condenser. In the following subsection a description of the modeling approach and the procedure adopted to predict the performance of a condenser is discussed.

FIGURE 1: Photograph of the Coils in a Lyostar II Condenser with non-uniform ice buildup

Modeling Approach

The DSMC solver SMILE (Statistical Modeling in Low density Environment) is used for all calculations [16]. In brief, the steps involved in setting up a case in SMILE involves the following. Generating the 3D DSMC surface mesh, assigning the surface properties, defining the jet of molecules, defining the chemistry model and the data file. More details have been provided in Ref. [16].

A low-temperature VHS water vapor molecular model with molecular mass 2.99e-26 kg and a molecular diameter 3.9Å was used. Unit thermal and momentum accommodation coefficient were applied to the coils and the housing. To simulate the vapor condensation process, the panels on the coils were assigned a unit sticking coefficient while the panels on the chamber were assigned to 0. A number of modifications to the gas-surface interaction procedure have been implemented to simulate the ice accretion process. These are described below.

Ice Accretion on the Coils

A freeze-drying cycle can last for 3 days. For a cycle with 100 vials, drying at 0.5 g/hr, this leads to the formation of 3.6 kg of ice. This corresponds to a total volume of 3871 cm^3 for a density of 930 kg/m^3 of ice. If the ice build-up is assumed to be uniform on the coils of the Lyostar condenser, a layer of ice about 1 cm thick is formed. In reality, the coils closest to the duct exit receive about twice as much ice as those farthest away from it.

The non-uniform ice growth can lead to a significant drop in the vapor trapping capability of the condenser. Kobayashi [15] showed that the decrease in performance of a condenser with ice formation in the coils is significant, and increases with reducing condenser temperatures. In order to predict the ice accretion on each coil during a cycle, a Gaussian weighted approach is used. Each node in the surface mesh is a part of 1 or more panels. If the distance between the node whose initial position is P_n^t and the centroid of the panel of which it is a part of is d, to predict the position of the node after time Δt we use the following

$$P_n^{t+\Delta t} = P_n^t + \frac{\sum_{N_P} \dot{m} N_n W}{N_P \times \rho_{ice}} \tag{3}$$

where N_p represents the number of panels connected to the point m, the steady state mass flux across the panel, N_n is the outward surface normal from the panel and W represents the Gaussian weight given to the panel based on the distance of the point d from the centroid of the panel. The weight is calculated as represented by

$$W = \frac{e^{-d^2}}{\sum_{N_P} e^{-d^2}} \tag{4}$$

Thus, in order to represent the ice buildup, each node is displaced through a distance proportional to the mass flux that was calculated using the DSMC simulations at a given node and along the direction of the outward surface normal of the panel the node is a part of.

Performance Metrics

In view of the requirements of a condenser discussed earlier, its performance can be evaluated based on a) the energy requirements for a cycle or the drying rate and b) the non-uniformity of ice formation on the coils. Condensers used today are bulky and the large volumes occupied by the condensing surfaces require an appropriate quantity of heat transfer fluid to condense the vapor completely. It is critical that the condenser efficiently traps the vapor that exits from the duct and prevents increase in the vapor pressure. Thus, it is desirable to have a higher area

averaged mass flux $\overline{m}$ on the condensing surfaces. It is equally important to evaluate the compactness of the condenser. Thus, the measure of efficiency for a condenser is the area averaged mass flux per unit volume $\overline{m_v}$ occupied by the condensing surfaces. Once the mass flux across the nodes are computed from the DSMC simulations, each of the panels are assigned a flux that is the average of the nodes it is composed of. The area averaged mass flux per unit volume of the condenser is computed as shown.

$$\overline{m_v} = \frac{\sum_i A_i \dot{m}_i}{AV} \tag{1}$$

where m_i is the mass flux across the panel i with an area A_i, A is the total surface area exposed for condensation and V is the volume occupied by the condensing surfaces.

Uniformity of ice formation is vital for the efficient usage of the condensing surfaces. Moreover, non-uniformities can lead to an uncontrolled increase in the water vapor pressure during the cycle resulting in a collapsed product. Hence it is extremely important to use the non-uniformity as a measure of the performance of a condenser. The measure of non-uniformity is defined as a ratio of the range in the mass flux to the area averaged mass flux as

$$Non-Uniformity = \frac{Range}{\overline{m}} \tag{2}$$

RESULTS

The primary factors that determine the performance of the condenser are a) the geometry and b) the presence of non-condensable gases in the chamber. Here, we compare two different geometries based on performance metrics defined earlier. The two designs simulated here are a) a laboratory scale FTS Lyostar II dryer and b) a conical design. The simulations discussed in this subsection are based on an inlet pressure of 8 mTorr, while the coils were maintained at -60 C, the chamber housing being insulated, was maintained at 0 C. While the Lyostar model had 48,000 panels, the conical design had 12,000 panels. The simulations were run on 8 CPUs of the SunFire4800 parallel computing server and the compute time was between 1-4 days. While the number of molecules at steady state in the Lyostar design was 760,000, the conical model had 1.6 million molecules.

Mass Flux in the Condenser Chamber: Lyostar II

As the vapor exits the duct, it expands, accelerating to velocities of ~400-500 m/s. In the Lyostar dryer, as the vapor exits the duct, it splits into two streams, symmetrically about the XY plane as shown in figure 2. The figure shows one half of the geometry with the coils close to the inlet and facing it receiving a higher flux compared to those that are further away. The flux on the coil closest to the inlet receives a flux that is ~2.5 times higher than on the coil that is farthest away from it.

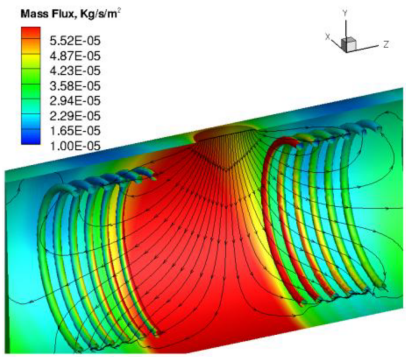

FIGURE 2: Mass flux contours superimposed with the streamtraces in the Lyostar II dryer

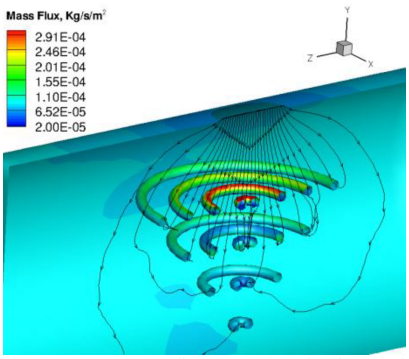

FIGURE 3: Mass flux contours in the conical dryer superimposed with the streamtraces

Mass Flux in the Condenser Chamber: Conical Design

In the conical design, the jet remains confined close to the duct exit and the presence of the condensing surfaces in the path of the vapor increases the mass flux on the coils significantly over the Lyostar. However, the mass flux reduces moving away from the duct, both radially and longitudinally. Figure 3 shows one half of the geometry along with the contours of mass flux on the coils with the streamtraces superimposed. The mass flux on the coils farthest

away from the duct exit reduces to a third of the value close to the duct exit. The conical design traps a significant portion of the flux that was lost to the walls of the chamber housing close to the duct exit in the Lyostar design. Thus, a 3 times increase in the area averaged mass flux on the coils of the conical design is observed.

Pressure and Velocity Contours in the YZ Plane

Figure 4 illustrates the pressure variation in the YZ plane for the two designs. The left half of the figure represents the pressure contours in the Lyostar while that on the right represents the contours in the conical design. The pressure in the conical chamber is higher than that in the Lyostar design. Thus, even though the conical design is efficient because it traps a higher on coming mass flux, the total surface area exposed is incapable of maintaining a pressure as low as that maintained by the Lyostar. Figure 5 represents the contours of average velocity in the YZ plane for the two designs. The jet expands as it enters into the chamber and reaches a velocity of ~450 m/s. However, the region of higher velocity for the conical condenser is confined to the region above the first set of coils. The coils being directly in the path of the vapor, obstructs it, leading to a high mass flux on the coils close to the inlet. However, moving radially outwards or in the shadow of the first set of coils, the flux reduces significantly.

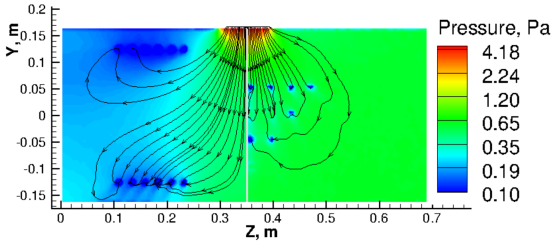

FIGURE 4: Pressure contours in the YZ plane for the two condenser designs in the YZ plane

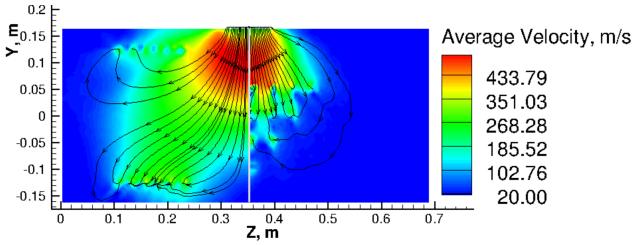

FIGURE 5: Average velocity contours for the two condenser designs

Performance Comparison

A summary of the performance of the two designs is shown in the Table 1. It was found that the $\overline{m}$ on the conical design was ~3.2 times that on the Lyostar condenser. Moreover, the $\overline{m}_v$ of the conical condenser increases by 8.5 times. However, from the pressure contours it was found that the least pressure that could be maintained in the conical condenser was twice that in the Lyostar chamber. This proves that while the conical design could be a useful, compact condenser design due to the large $\overline{m}$ and $\overline{m}_v$, it may not be able to maintain the same pressure levels as is maintained by the Lyostar dryer. In the conical design, the presence of the coils in the shadow of the first row increases the non-uniformity as these coils receive a significantly lower mass flux compared to the first row. Thus, we see a 40% increase in the non-uniformity over the Lyostar design.

TABLE 1. Comparison of performance between the Lyostar and conical condensers

Design	Lyostar II	Conical	Change of Conical compared to Lyostar
$\overline{m}$, kg/s/m^2	3.27e-5	10.18e-5	3.2 times increase
$\overline{m}_v$, kg/s/m^2 /m^3	0.026	0.22	8.5 times increase
Non-uniformity,%	264	371	40.5% increase

Verification of Ice Accretion Simulations

A comparison was made with the analytical solution for flow of water vapor over a cylinder in free molecular flow. Using the inward number flux on the surface of a cylinder of radius 2 cm and with the following parameters for the analytical solution, the ice growth for a period of 1 hour was compared to that predicted using the algorithm. Density of ice: 930 kg/m^3, free-stream velocity: 400 m/s, free-stream temperature: 213 K, pressure: 6 mTorr, speed ratio: 0.9, sticking coefficient:1

Figure 6 shows the comparison between the analytical solution and the predicted ice growth. It is clear that the predicted profile matches the analytical solution quite well and the observed deviation can be attributed to the grid resolution used.

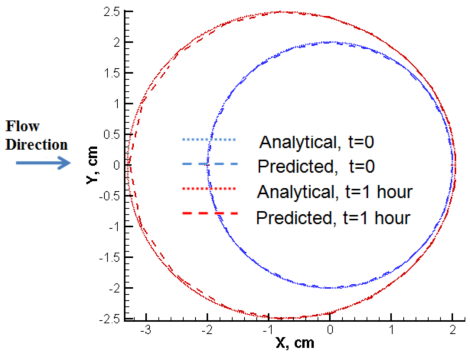

FIGURE 6: Comparison between the analytical solution and the predicted ice growth over a period of 1 hour

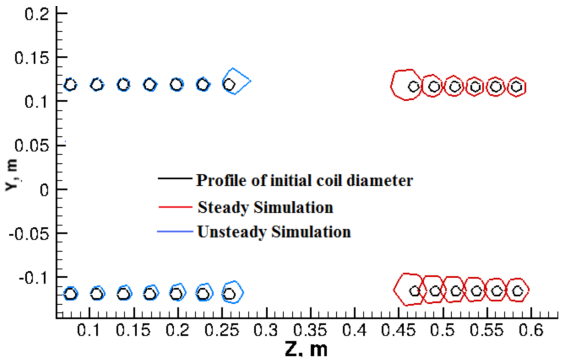

FIGURE 7: Comparison of the steady and unsteady non-uniform ice buildup on the Lyostar dryer

Prediction of Ice Accretion on the Coils of the Lyostar Condenser

With the predicted mass flux discussed earlier, we expect the ice accumulation on the coils close to the duct exit to be higher than that on the coils away from it. Figure 7 represents the steady and unsteady prediction of the ice accumulated on the coils in the YZ plane over a period of 75 hours. In the steady simulation, the coils close to the duct exit have a maximum ice accumulation of 2.2 cm over a period of 75 hours while that on the coils farthest away from the duct exit have a thickness of 0.5 cm. Figure 8 illustrates the steady state 3D prediction of the ice growth.

The ice accretion profile obtained from the steady state mass flux computed across the DSMC surface mesh was found to under predict the non-uniformity. This was attributed to the unsteady nature of the ice accretion. Thus, the single update of the geometry was replaced by an updated geometry, with a new surface mesh after ice thickness equal to 15% of the initial coil diameter had accumulated on the coils. The DSMC simulation was then re-run on the new geometry and the ice accretion profile was then recalculated after another 25 hours of the drying process under the same conditions. The predicted growth was found to be extremely non-uniform with the coils closest to the duct exit receiving 2.2 cm of ice formation but that farthest away merely 0.1 cm (Figure 9). While the contours provide a useful means of estimating the variation in the ice thickness over individual coils apart from the variation from one coil to the other, future efforts will focus on studying convergence in the ice accretion profile using unsteady techniques.

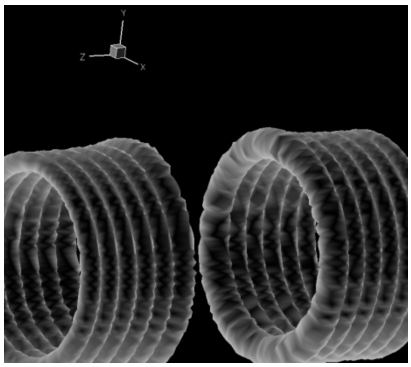

FIGURE 8: Steady prediction of 3D non-uniform ice buildup on the Lyostar condenser

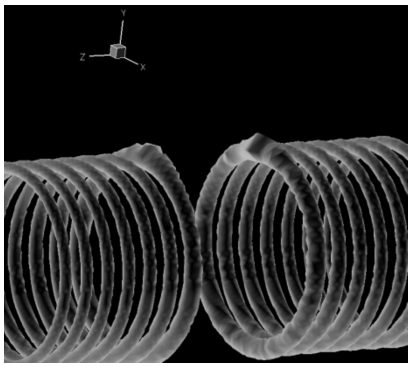

FIGURE 9: Unsteady prediction of the ice buildup on the coils of the Lyostar condenser

CONCLUSIONS

The current work focuses on using DSMC techniques to model the vapor flow in the condenser of a pharmaceutical freeze-dryer. Relevant metrics for comparing condenser performance are defined. These metrics were used to compare the performance of two condenser designs, the Lyostar II and the conical design. It was found that while the least pressure that could be maintained in the conical condenser was twice that in the Lyostar, the $\overline{m}$ was ~3.2 times higher and the $\overline{m}_v$ was 8.5 times higher. Thus, while the conical design could be a useful, compact condenser design, it may not be able to maintain the same pressure levels as is maintained by the Lyostar dryer. Moreover, the presence of the coils in the shadow of the first row increased the non-uniformity as these coils received a lower mass flux compared to the first row. There was a 40% increase in the non-uniformity over the

Lyostar design. The steady state mass flux was used to predict the development of the ice front on the condenser coils. To verify the algorithm used for the prediction, a comparison was made with an analytical solution for the condensation of vapor during free molecular flow around a cylinder. It was found that the coils closest to the vapor inlet were subjected to the largest mass flux, leading to accumulation of ice around these coils. The thickness of the ice formed on the coil closest to the duct exit was 2.2 cm while that on the coil farthest from it was 0.5 cm over 75 hours. The non-uniformity was under predicted compared to the experimental measurements discussed in the introduction. This was attributed to the unsteady ice accretion. For unsteady ice build-up calculations, a new surface mesh was used after ice thickness reached 15% of the initial coil diameter. The unsteady simulations predict a much higher non-uniformity in ice growth with the coils closest to the duct exit having about 20 times larger ice growth rate than the coils at the far end.

From the experimental observations, it was noticed that there may be a non negligible difference between the inlet and exit temperatures of the coil. However, since this temperature variation was not known, in the modeling, it was assumed that all the coils were at a uniform temperature and hence were prescribed a unit sticking coefficient. The non-uniformity of ice buildup can be attributed to two aspects, a) the flow structure and b) the temperature variation in the coils between the inlet and outlet. While the current technique captures the non-uniformity due to the former, future efforts will focus on prescribing a known mass flux across the duct based on the experimental measurements and capture the ice formation based on the temperature dependent sticking coefficient as well to accurately represent ice formation based on multiple updates of the coil geometry.

ACKNOWLEDGMENTS

The financial support from National Science Foundation, CBET/GOALI-0829047, Baxter BioPharma LLC and Purdue's Center for Advanced Manufacturing is gratefully acknowledged. The authors would also like to thank Drs. Wei Kuu and Gregory Sacha of Baxter Bloomington for extremely useful discussion of freeze-drying hardware.

REFERENCES

1. A. Alexeenko, A. Ganguly, and S. L. Nail, *J. Pharma. Sci.*, **246**, 1–12, (2002).
2. F. Franks and T. Auffrett. "Freeze-drying of Pharmaceuticals and Biopharmaceuticals". (RSC, Cambridge, 2007).
3. Y.G. Liu, Y. Zhao and X. Feng. *Appl. Thermal Engr.*, **28**, 675–690, (2008).
4. J. M. Flink. *Food Tech.*, **31**, 77–84, (1977).
5. Ratti. *J. Food Engr.*, **49**, 311–319, (2001).
6. É. I. Guigo and D. Tsvetkov, J. of Engg. Physics and Thermophysics, 23 (5), 1422 (1972).
7. A.V. Luikov and D.P. Lebedev, Intl. Journal of Heat and Mass Transfer, 16 (6), 1087-1090, (1973).
8. T. A. Jennings. *Lyophilization: Introduction and Basic Principles*. (Interpharm CRC, New York, 2002).
9. D.P. Lebedev, J.of Engg. Physics and Thermophysics, 21 (2), 1013-1018 (1971).
10. T. Tachiwaki, M. Muraoka, K. Sawada and H. Uyeha, Vacuum, 41 (7-9), 2038-2040, (1990).
11. H. Kramers and S. Stemerding, 3 (1), 73-82, (1951).
12. G. Oetjen and P. Haseley. Freeze-Drying. (Wiley-VCH, Weinheim, Germany, 2004).
13. Kobayashi M. "Important Problems in freeze-dryers: Mainly on the vapor removing performance and its control". In IIF-IIR-Commission c1, Tokyo, Japan, (1985).
14. Kobayashi M. "Development of a new refrigeration system and optimum geometry of the vapor condenser for pharmaceutical freeze dryers". In Proceedings of the 4th International Drying Symposium, Kyoto, Japan, (1984).
15. G. Oetjen, L. Rey, and J. C. eds. May. *Freeze-drying/Lyophilization of Pharmaceutical and Biological Products*. (Marcel Dekker, Inc, New York, 1999).
16. M.S. Ivanov, *et al*. "Smile system for 2d/3d DSMC computations, proceedings of 25th international symposium on rarefied gas dynamics". *In Proceedings of 25th International Symposium on Rarefied Gas Dynamics*, St. Petersburg, Russia, (2006).